

## **CuSe<sub>1-x</sub>S<sub>x</sub> nanosheets with an ordered superstructure as anode materials for lithium-ion batteries**

Chunshuang Yan, Gang Chen,\* Yongqiang Zhang, Dahong Chen, Jian Pei and Zhuangzhuang Qiu.

### **Experimental**

#### **Materials synthesis**

All chemicals were purchased from the indicated suppliers and used without any further purification. In a typical synthesis of ternary CuSe<sub>1-x</sub>S<sub>x</sub>, Na<sub>2</sub>SeO<sub>3</sub> (0.5 mmol), Cu(CH<sub>3</sub>COO)<sub>2</sub>•H<sub>2</sub>O (1 mmol) and NaOH (0.2 g) were dissolved into the mixed solvent of H<sub>2</sub>O (18 ml) and ethylene glycol (10 ml) by vigorous stirring. Then the 2 ml of thioglycolic acid was added into the solution and stirred for another 10 min. The prepared solution was transferred into a Teflon-lined stainless steel autoclave with a capacity of 40 ml. Subsequently, 2 ml of hydrazine (80%) was added into the autoclave, which was then sealed and held in the oven at 140 °C for 12 h. After the autoclave cooled to room temperature naturally, the synthesized products were collected, centrifuged and then washed with deionized water and ethanol several times, and finally dried in a vacuum at 60 °C for 12 h for further characterization.

#### **Materials characterization**

Powder X-ray diffraction (XRD, recorded on a Bruker D8 Advance X-ray diffractometer equipped with Cu K $\alpha$  radiation ( $\lambda = 1.5408 \text{ \AA}$ )) was employed to characterize the crystalline structure of the samples. The morphologies of the obtained samples were investigated by a field emission scanning electron microscopy (SEM, FEI Quanta 200F) and transmission electron microscopy (TEM, FEI Tecnai G2 S-Twin). Surface analysis was detected on X-ray photoelectron spectroscopy (XPS) with an Al K $\alpha$  chromatic X-ray source (1486.60 eV, PHI 5700 ESCA System, USA).

#### **Lithium storage performance**

The active material ( $\text{CuSe}_{1-x}\text{S}_x$ ), conductivity agent (acetylene black), and polymer binder (poly(vinylidene fluoride), PVDF) were mixed at a weight ratio of 80:10:10 and dispersed in a N-methylpyrrolidone (NMP) solution to form a homogenous slurry. The slurry was coated onto the copper foil substrates and dried in a vacuum oven for 12 h at 120 °C. The prepared copper foil was cut into small circle strips and pressed at 6 MPa before coin cell assembly. The cells (CR2032 type coin cells) were assembled in a glove box filled with ultra-high purity argon using polypropylene membrane as the separator, lithium metal as the anode, and 1M  $\text{LiPF}_6$  solution in ethylene carbonate (EC)-diethyl carbonate (DMC) (1:1 *V/V*) as the electrolyte. The charge and discharge performance of the electrodes was evaluated using a battery test system (Neware BTS-610) between 0.01 and 3 V. The cyclic voltammetry (CV) measurements and electrochemical impedance spectroscopy (EIS) were performed on a CHI604C electrochemical workstation.

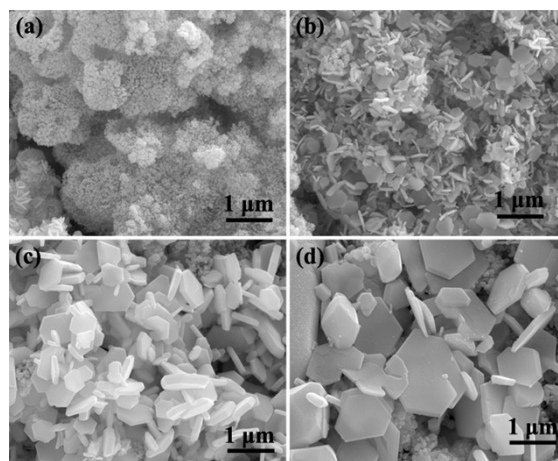


Fig. S1 The morphologies of the  $\text{CuSe}_{1-x}\text{S}_x$  crystals synthesized in an EG and water mixture with a 10:18 volume ratio for different time intervals: (a) 1 h, (b) 2 h, (c) 4 h and (d) 8 h.

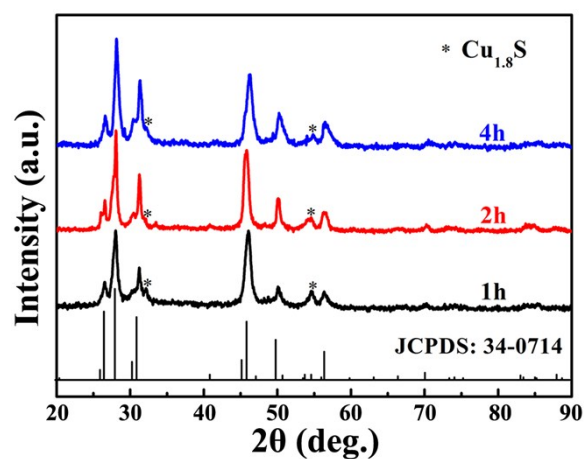


Fig. S2 The XRD patterns of the  $\text{CuSe}_{1-x}\text{S}_x$  crystals synthesized in an EG and water mixture with a 10:18 volume ratio for different time intervals: 1 h, 2 h and 4 h.

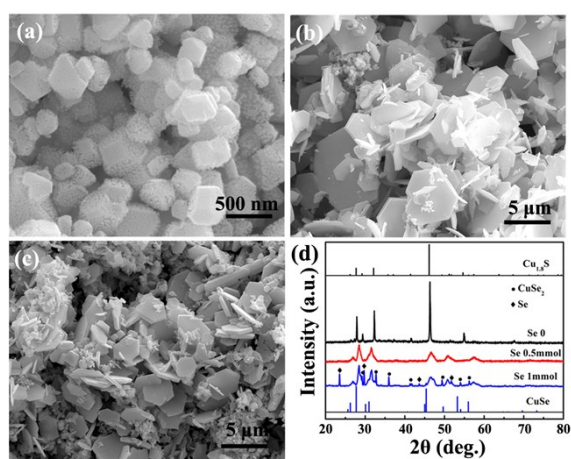


Fig. S3 The SEM images of the products with different amounts of  $\text{Na}_2\text{SeO}_3$ : (a) 0 mmol, (b) 0.25 mmol, (c) 1 mmol and (d) The corresponding XRD patterns.

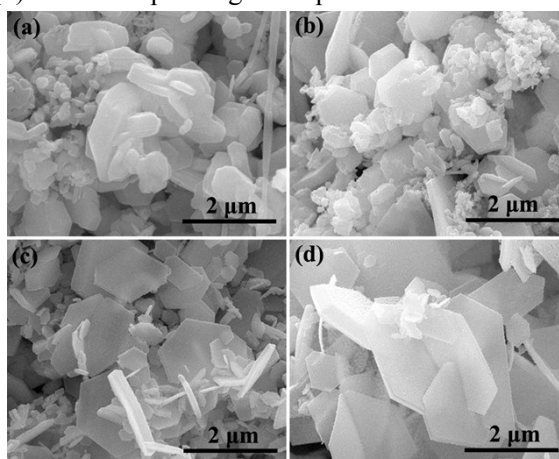


Fig. S4 The SEM images of the products with different solvent ratio (ethylene glycol/ $\text{H}_2\text{O}$ ): (a) 28:0, (b) 18:10, (c) 8:20 and (d) 0:28.

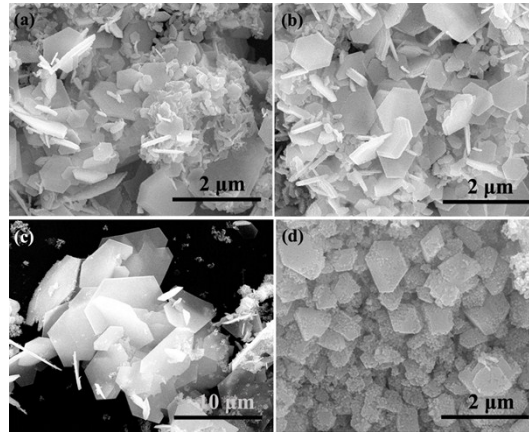


Fig. S5 The SEM images of the products with different amounts of NaOH: (a) 0 g, (b) 0.1 g, (c) 0.4 g and (d) 0.8 g.

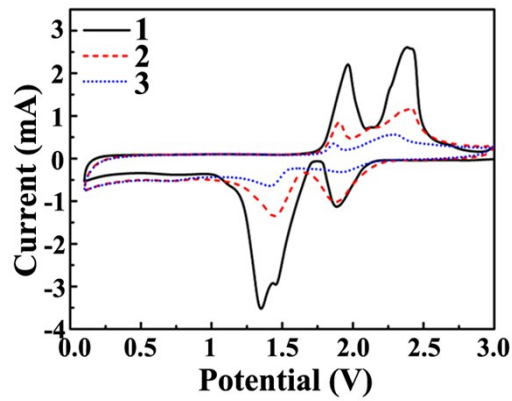


Fig. S6 CV curves of the as-formed ordering  $\text{CuSe}_{1-x}\text{S}_x$  NSs in the first three-cycles at a scan rate of  $0.5 \text{ mV s}^{-1}$ .

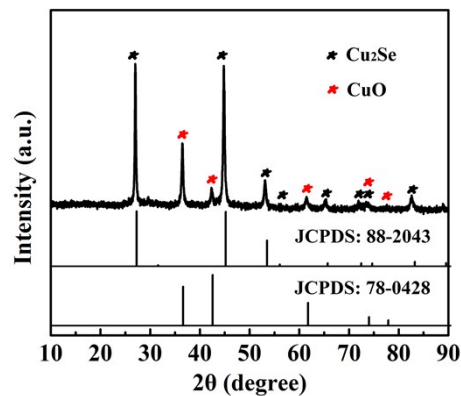


Fig. S7 The XRD pattern of the as-prepared  $\text{Cu}_2\text{Se}$  under no adding sulphur source and keeping other conditions unchanged.

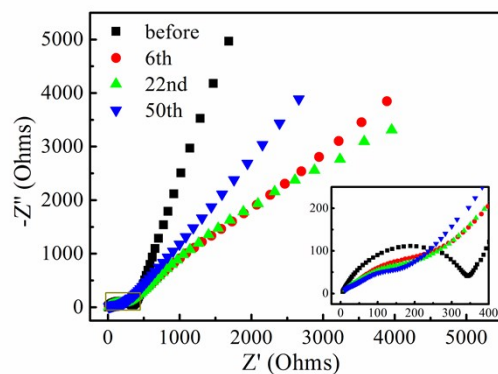


Fig. S8 The electrochemical impedance spectroscopy (EIS) for raw and 6th, 22nd, 50th cycles.

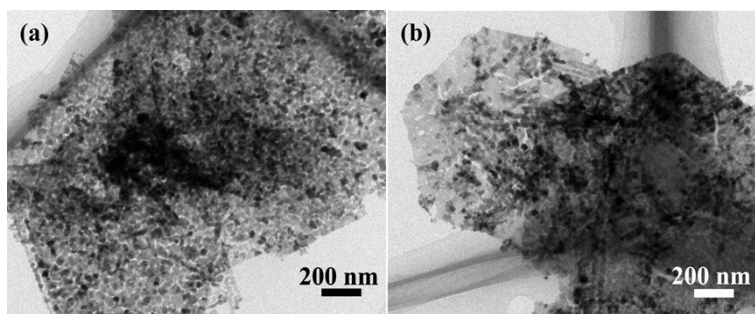


Fig. S9 (a, b) TEM images of as-formed ordering  $\text{CuSe}_{1-x}\text{S}_x$  NSs at a current density of  $50 \text{ mA g}^{-1}$  after cycling for 60 cycles.

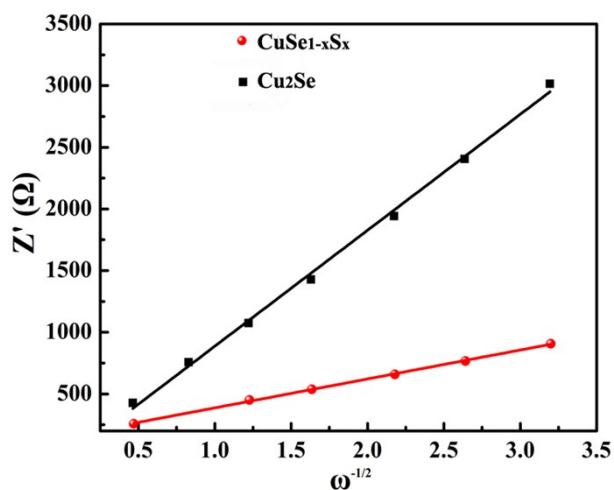


Fig. S10 The  $Z' - \omega^{-1/2}$  plots for the  $\text{CuSe}_{1-x}\text{S}_x$  and  $\text{Cu}_2\text{Se}$  electrodes obtained after charge/discharge cycling test, indicating that the  $\text{CuSe}_{1-x}\text{S}_x$  has a smaller  $\sigma$  value than the  $\text{Cu}_2\text{Se}$ .

We calculate Li ion diffusion coefficient ( $D_{Li}$ ) of ordering  $CuSe_{1-x}S_x$  NSs and  $Cu_2Se$  from the Nyquist plots after charge/discharge cycling test according to the following formulas:

$$Z' = R_{ct} + R_s + \sigma\omega^{-1/2}$$

$$D_{Li} = R^2 T^2 / 2 A^2 n^4 F^4 C_{Li}^2 \sigma^2$$

Where  $Z'$  is the real component of the impedance and has a linear relationship with  $\omega^{-1/2}$  ( $\omega$ , angular frequency);  $\sigma$  is the warburg factor and obtained from the slope of the  $Z' - \omega^{-1/2}$  line. One can see that the ordering  $CuSe_{1-x}S_x$  NSs electrode has a smaller  $\sigma$  than the  $Cu_2Se$  electrode ( $234\Omega \text{ rad}^{1/2} \text{ s}^{-1/2}$  for the former and  $940\Omega \text{ rad}^{1/2} \text{ s}^{-1/2}$  for the latter). Thus, the ordering  $CuSe_{1-x}S_x$  NSs electrode has a bigger Li ion diffusion coefficient. In other words, we indicate that the ordered superstructure can improve Li ion diffusion qualitatively by calculating warburg factor  $\sigma$ .